Estimation of the light output power and efficiency of a XeCl dielectric barrier discharge exciplex lamp using one dimensional drift-diffusion model for various voltage waveforms

T. Doanh LE
Dr
Laboratoire LAPLACE
Université Paul Sabatier,
118 Route de Narbonne,
31062 Toulouse, France
lethanh@laplace.univ-tlse.fr

Sounil BHOSLE
Dr.
OLISCIE
175, chemin de la Pielle
31600 Lherm, France
sounil.bhosle@oliscie.com

Georges ZISSIS
Professor
Laboratoire LAPLACE
Université Paul Sabatier,
118 Route de Narbonne,
31062 Toulouse, France
georges.zissis@laplace.univ-tlse.fr

Hubert PIQUET
Professor
Laboratoire LAPLACE
Université Paul Sabatier,
2 Rue Charles Camichel,
31071 Toulouse, France
hubert.piquet@laplace.univ-tlse.fr

Abstrat: **A XeCl dielectric barrier discharge under applied pulsed and sinusoidal voltage waveforms is simulated using a one dimensional drift diffusion model. In both waveforms, the light output depends not only on the gas mixture composition but also on the electrical parameters of the voltage waveform such as the frequency, the duty ratio…ctc. At the same amplitude of the voltage and the frequency, the UV output efficiency of the pulsed voltage is higher than the one of sine voltage. These results obtained in this paper allow to find out an appropriate power supply mode for a DBD excilamp.**

***Index Terms*: Dielectric barrier discharge; Excimer; Exciplex, excilamp; Ultra-violet; UV radiation; VUV radiation**

I. INTRODUCTION

An exciplex lamp operated using dielectric barrier discharges (DBDs) is one of the most powerful ultra-violet (VUV or UV) light sources. In recent years, the DBD UV light sources have been widely used in several industrial applications as well as in lighting and medical technology.

A primary feature of the excilamp is that the dielectric barrier suppresses the occurrence of an arc discharge and the damages to the metallic electrodes. Furthermore, the lamp can provide various wavelengths of narrow band UV light.

Depending on the gas composition and conditions under which an electric discharge occurs, excited molecules are produced by different mechanisms (the harpoon reaction and ion-ion recombination) with characteristic radiative life time of 10^{-7}-10^{-9}s. Spontaneous decay of excimer and exciplex molecules into individual atoms is accompanied by emission of a UV light. In this UV field, dielectric barrier discharges in rare gas or halide/rare gas mixtures are promising. These discharges are usually made of a silica gas chamber, including the gas or gas mixture at a pressure between 10^4Pa and 10^5Pa, with outer electrodes. Up to now, a number of research groups have in detail investigated UV light emission from exciplex excited using DBD plasma experimentally [10][5][6][13]. They reported that the experimental values of the UV light output efficiency were around 15% although the theoretical ones may be several tens of percent.

Xenon/Chlorine excilamps are used in skin treatment: such a gas mixture has very interesting specificity as it emits almost exclusively in the UVB range (280nm-315nm). This radiation affects the immune system and has an especially high efficiency for curing affectations due to the over activity of this system, such as psoriasis and vitiligo.

In the present paper, in order to find out optimum voltage waveforms for further improvement of the excilamp characteristics, we take pulse and sinusoidal waveforms for source voltage. We simulate XeCl DBD plasma using a one dimensional drift diffusion model in which the approximation of the local electrical field has been applied.

Basing on this developed model, we compare the dependence of the UV light output power and efficiency of the XeCl excilamp on the applied pulse and sinusoidal voltage waveforms. The influence of the waveform parameters of both voltages such as the frequency, the duty ratio, the rising time of a pulse voltage and also the gas composition such as the ratio of chlorine and the total pressure on the production of the UV have been investigated in detail.

II. MODELING

A. Drift diffusion model

The gas pressure in which the discharge is established is in the case of DBDs for UV production, between 10^3 and 10^5Pa, which makes that plasma strongly collisionnal. In those conditions, the directed energy of the particles can be neglected compared to their random motion energy (thermal energy). This collisional behavior causes the temporal variations of the studied variables (densities, fluxes, temperatures…) to be much lower than the momentum exchange frequency by collision. This leads to strong simplifications of the momentum conservation equation. With additional approximations (scalar pressure, etc…), the flux of particles can be written:

$$\vec{\Gamma}_s = \text{sign}(q_s) n_s \mu_s \vec{E} - D_s \vec{\nabla} n_s \quad (1)$$

With: q_s: elementary charge of the specie s

n_s: density of the specie s. It depends on the position $\vec{r}$ and the time t

μ_s: mobility of the species

D_S: diffusion coefficient of the specie s

$\vec{E}$: Electrical field

The first term on the left of the equation is related to the electrical field which corresponds to the drift motion of the particles (provided they have a charge). The second one corresponds to the diffusion motion which is a collisional effect which tends to uniformize the density. Including the expression of that flux in the mass conservation equation leads to the following drift –diffusion equation:

$$\frac{\partial n_s}{\partial t} + \vec{\nabla}.(-D_s \vec{\nabla} n_s \pm \mu_s n_s \vec{\nabla} V) = S_s \quad (2)$$

With: V: electrostatic potential

S_s: source term for the specie s

In spite of the previous simplifications, the system made of the coupling of the equation 2 written for all species considered in the plasma is still not closed. Indeed, some variables are still undefined.

In order to get rid of the indetermination of the electrical field, Poison's equation can be coupled to the system but a further approximation is needed to get the transport coefficient μ_s and D_s.

B. Approximation of the local field

The energy gained by electrons in the electrical field during an infinitesimal lapse of time is assumed exactly balanced by their collision energy losses. This is valid for a plasma in which the electrons have a collision frequency high enough to be in equilibrium with the electrical field. In that case, their distribution function only depends on the local electrical field $\frac{\vec{E}}{N}$ (where N is the density of all gas atoms). Consequently, the collision frequencies, the mobilities and the diffusion coefficients depend as well exclusively on the electrical field.

One important implication of using the local field approximation is that the energy balance equation is not computed, reducing significantly computing resources. The counter part is that powers (radiatives and electric) are not quantitatively computed. This explains the sums of radiative efficiencies above 1 in section D. However, the optimal points are conserved, which is the focus of this work dedicated to the identification of optimal parameters for a DBD excilamp power supply.

III. GOVERNING EQUATION

Basing on the previous approximations, the phenomena of the plasma in the mixture of xenon and chlorine is governed by the following closed equation system (3).

This system contains a Poison's equation coupled to as many equations of all species considered in ours discharge. The subscript e, i^+ and i^- represent the electrons, the positive ions and the negative ions.

$$\begin{cases} \vec{\nabla}.(-\varepsilon \vec{\nabla} V) = e(n_{i+} - n_e - n_{i-}) \\ \frac{\partial n_e}{\partial t} + \vec{\nabla}.(-D_e \vec{\nabla} n_e \pm \mu_e n_e \vec{\nabla} V) = S_e \\ \frac{\partial n_{i+}}{\partial t} + \vec{\nabla}.(-D_{i+} \vec{\nabla} n_{i+} + \mu_{i+} n_{i+} \vec{\nabla} V) = S_{i+} \\ \frac{\partial n_{i-}}{\partial t} + \vec{\nabla}.(-D_{i-} \vec{\nabla} n_{i-} + \mu_{i-} n_{i-} \vec{\nabla} V) = S_{i-} \\ ..... \\ ..... \end{cases} \quad (3)$$

After all those approximations, the studied plasma is governed by a coupled Partial Differential Equation (PDE) system which can be numerically solved on a spatial domain Ω limited by a surface $\partial\Omega$ provided:

- The values of the transport coefficients (motilities, diffusion coefficients) and the source terms are known as a function of the local electrical field.
- The boundary conditions are clearly defined included.

A. Boundary conditions for the species s

The boundary conditions for all species considered in our model such as electrons, positive and negative ions and the excited atoms or molecules are the same as those in our previous paper [Bh-1].

B. Boundary condition for Poison's equation

The continuity of the potential involves a constraint on the metallic electrodes on the outside face of the dielectrics (Dirichlet conditions). This kind of boundary condition allows us to define the applied voltage on the DBD. For example, if the DBD is applied with a sine or pulse wave form at 50 kHz and with maximum amplitude of 8kV, the boundary condition will be:

Electrode 1: V = 0

Electrode 2: $V = 8000\sin(2\pi.50\times10^3 t)$.

C. Reaction processes and coefficient transport

The reaction processes among electrons, positive and negative ions of xenon and chlorine, excited atoms of xenon and chlorine are took from the literature [4],[7],[8],[9],[11], [12] et [14]. The frequency of collision and the coefficient of direct ionization for chlorine and xenon are calculated by the software of Bolsig+ [3].

The coefficient of absorption, desorption and recombination on the dielectric surface are the following values:

$K_{adse} = K_{adsi-} = K_{adsi+} = 10^{12}$ (s^{-1}), $K_{des} = 10^{7}$ s^{-1} and $K_{rec} = 10^{-12} m^3.s^{-1}$.

IV. RESULTS AND DICUSSION

A. *Geometry of the model*

The model is solved in a geometry corresponding to [2] and [12], which means a homogeneous discharge between two plane electrodes covered with the dielectrics (with a relative permittivity equal to 4, which approximately corresponds to the silica glass). The model can be numerically solved in 1D using the software Comsol Multiphysics. The figure 1presents the discharge geometry and associated resolution domains. The resolution domain for all the species considered is between two points B and C, which corresponds to the discharge domain.

The inter –electrode space (discharge volume) is filled with the mixture of Xenon/chlorine at total pressure of 400Torr and the mixture ratio of Xe/Cl_2 = 97:03.

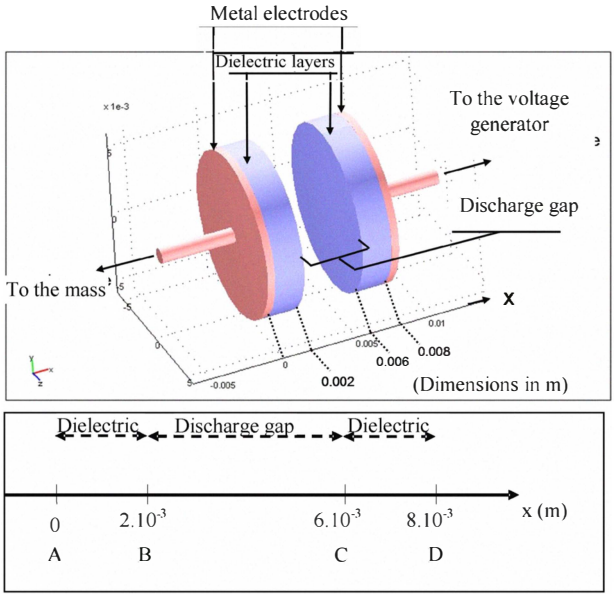

Figure 1. Discharge geometry and associated resolution domain

B. *Waveform of voltage and discharge current*

Figure 2 shows the following waveforms; $v_S(t)$, the power source voltage; $v_W(t)$ the voltage between the barriers; $v_G(t)$, the voltage in the gap and $i_T(t)$, the density current in the periodic steady state. It is shown that $v_W(t)$ is a major component in $v_S(t)$. The $v_W(t)$ waveform is similar to a sinusoidal wave, however, it increase rapidly at $\omega t = 0{,}14\pi$ and drops at $\omega t = 1{,}14\pi$ due to the appearance of sharp spikes in i_T (t). On the contrary the $v_G(t)$ waveform is distorted considerably, with two peaks at $\omega t = 0{,}12\pi$ and $\omega t = 1{,}12\pi$ and its fundamental wave leads $v_S(t)$ by $0{,}28\pi$. At ωt corresponding to the v_G peaks, sharp spikes in the $i_T(t)$ waveform appear, since the electron multiplication starts in the vicinity of the anode (see A and C in figure 9) and extends to the cathode (see B and D in figure 9). The $i_T(t)$ phase leads $v_S(t)$ by $0{,}35\pi$ and $v_G(t)$ by $0{,}17\pi$. This relation represents that this discharge is capacitive.

The spatial distribution of the potential at $\omega t = 0.5\pi$, π, 1.5π and 2π are shown in figure 2 (b). The voltage drops of the grounded and powered side barriers are equal at any phase, since the same barriers are utilized for both electrodes.

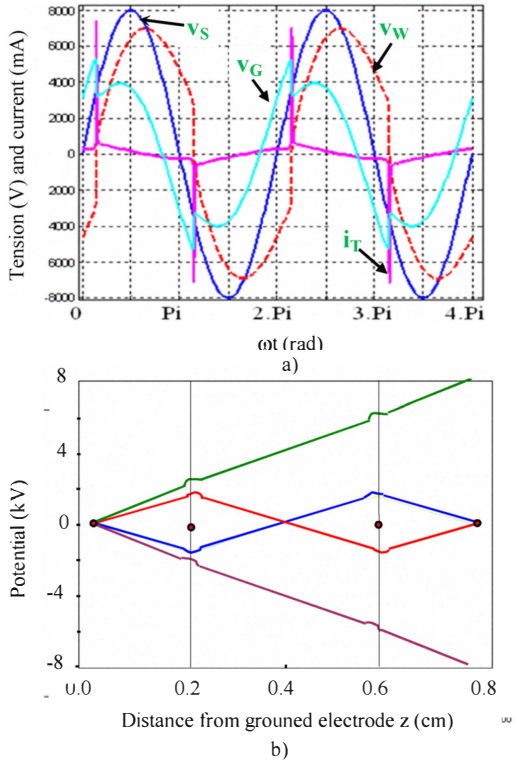

Figure 2: (a) Temporal variations of the source voltage $v_S(t)$, voltage in the gap $v_G(t)$, voltage between the barriers $v_W(t)$ and total current $i_T(t)$ under sine voltage waveform with f =50kHz, total pressure =400Torr, rate of mixture Xe/Cl_2 =97:03, V_s = 8kV; (b) Potential distributions between the electrodes for $\omega t = 0{,}5\pi$, π, 1.5π and 2π. Here the vertical lines at z=0.2cm and 0.6cm represent the barrier surfaces.

C. *Spatio-temporal profiles the discharge plasmas*

Figure 3 shows spatio – temporal profiles of (a) the electron concentration $n_e(z,t)$, (b) the electric field strength E(z,t), (c, d) the excimers concentration of Cl^*_2 and Xe^*_2 ($^3\Sigma^+_u$), and (e, f) the exciplexes concentration of $XeCl^*$ and Xe_2Cl^* for the sine waveform.

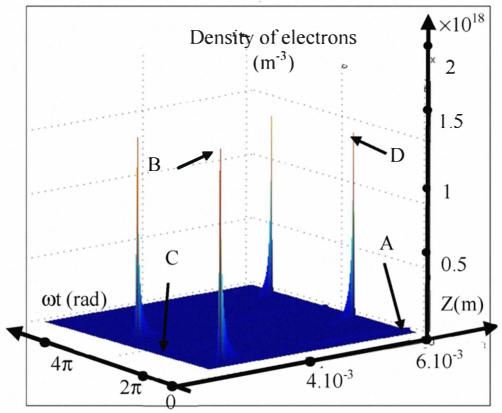

a)

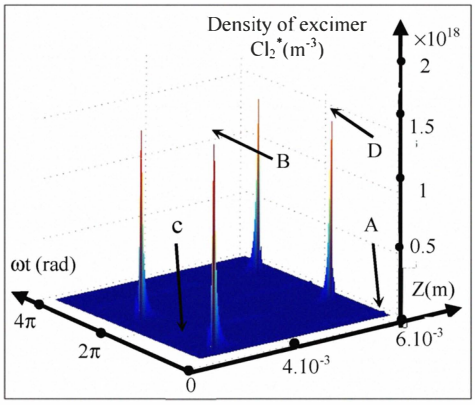

d)

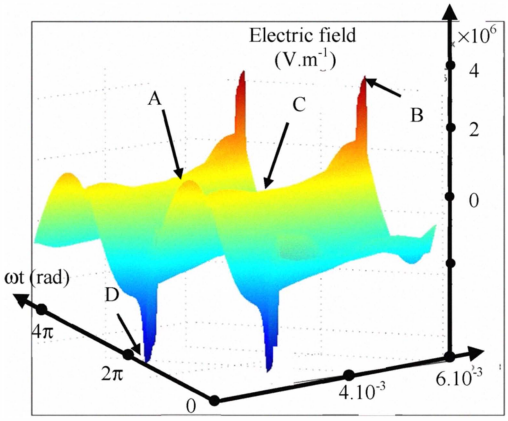

b)

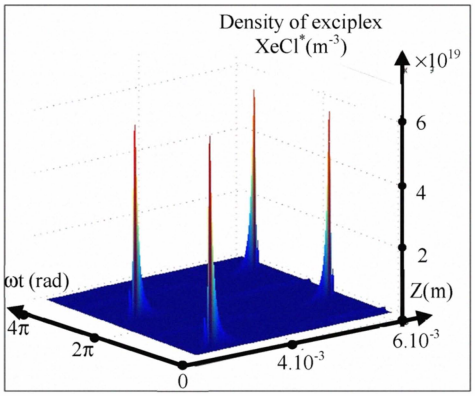

e)

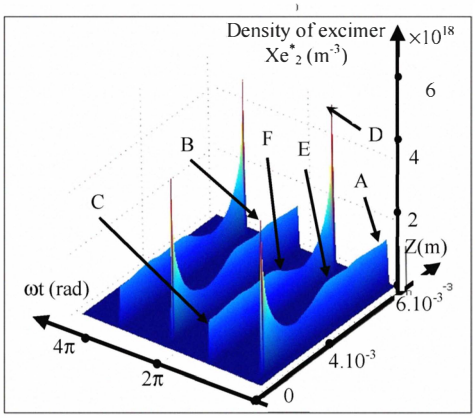

c)

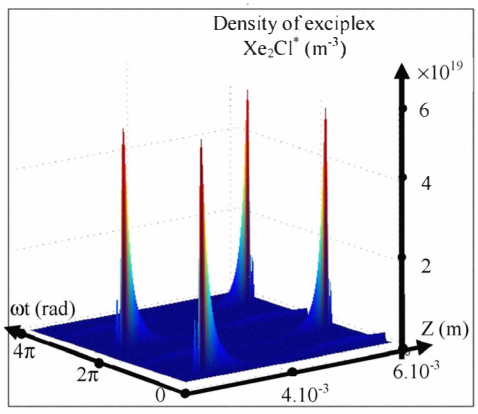

f)

Figure 3. Spatio-temporal profiles of (a) the electron concentration n_e, (b) the electric field strength E, (c, d) the Cl^*_2, Xe^*_2 ($^3\Sigma^+_u$) excimers concentrations, and (e, f) the $XeCl^*$, Xe_2Cl^* exciplexes concentration for the sine waveform with the maximal amplitude of 8kV, frequency = 50 kHz, total pressure = 400Torr and the mixture rate of Xe/Cl_2 = 97:03

Figures 3(a) shows that two peaks in n_e indicated by B and D appear at each a half cycle because of the electron multiplication. The n_e peaks appear always on the instantaneous cathode side defined by the polarity of v_G shown in figure 6. The n_e value in the volume of discharge (z=3mm, 4mm and 5mm) does not appreciably and reaches the following values: $4{,}6\times10^{16}m^{-3}$, $2{,}4\times10^{16}m^{-3}$ and $4{,}6\times10^{16}m^{-3}$ respectively.

Figure 3(b), E (z, t) at the barrier wall changes between ±44,6 kV cm^{-1}. The formation of the grounded side sheath is explained by the motions of electrons and total ions. A peak in E(z,t) at point B is also explained by the electron multiplication and n_{i+} peaks. However, the local distortion in E (z, t) appears at A and C due to the effect of the wall charge

During the period between two points A and B, the electron energy rises instantaneously all over the discharge space. Then, the electron multiplication occurs nearly the cathode site.

Figure 3 (c) shows that Xe^*_2 ($^3\Sigma^+_u$) is generated not only in the cathode side sheath but also in the bulk region, in which the electron multiplication is significant (see B and D in figure 3 (a)). In particular, two sharp peaks n_{Xe*2} at B, and D in the cathode sheath at $\omega t = 0{,}14\pi$ and $\omega t = 1{,}12\pi$ in a period are appreciably high and their magnitudes are about 6.10^{18} m^{-3}. The values of n_{Xe*2} at E and F in the region of discharge volume are $2\times10^{18}m^{-3}$ and $2{,}2\times10^{18}m^{-3}$.

Figure 3 (d) shows that the Cl^*_2 is similar to the profiles of $n_e(z,t)$ and n_{Xe*2} (z, t) but the peaks in n_{Cl*2} at A, B, C and D are much less than the ones of n_{Xe*2} (z, t).

Figure 3 (e, f) shows the evolution of the exciplexes $XeCl^*$ and Xe_2Cl^*. They are also similar to the electron density n_e and the excimers density of Xe^*_2 and Cl^*_2. The peak values of $XeCl^*$ and Xe_2Cl^* are mainly generated on the cathode site because of the electron multiplication. By comparing the maximal density between the excimers Cl^*_2 and Xe^*_2 ($^3\Sigma^+_u$) with the exciplexes of $XeCl^*$ and Xe_2Cl^* considered in our model, we note that the density of $XeCl^*$ is ≈1.5 times superior to that of Xe_2Cl^*, ≈ 21 times superior to that of Xe^*_2 ($^3\Sigma^+_u$), ≈ 32 times superior to that of Cl^*_2.

D. Efficiency of the UV output light emission

Our model of Xe/Cl2 excilamp developed in the previous part permit us to access directly the radiation of Xe^*_2 et Cl^*_2 exicmers as well as $XeCl^*$ and Xe_2Cl^* exciplexes at a point x and time t. The UV flux of photons Φ (x,t) emitted by the excimers and exciplexes is calculated as the following:

$$\Phi_i(x,t)=\sum K_i * n_{i(\text{excimers or exciplex})} \quad (4)$$

Here : K_i : Radiative dissociation rate of excimer or exciplex

n_i : Density of an excimer ou exciplex

Consequently, the radiated power emitted by the discharge and the instantaneous electric power at time t is:

$$P_{i\_radiation}(t)=Sh\nu_i \oint_0^L \Phi_i(x,t) \quad (5)$$

$$P_{i\_elec}(t) =SV_D(t)j_T(t) \quad (6)$$

Here :

h : Planck's constant ($6{,}626.10^{-34}$J.s)

ν_i: Frequency of a photon at 172nm ($1{,}74.10^{15}$ Hz), 308nm ($9{,}74.10^{14}$ Hz) and 490nm ($2{,}04.10^{14}$ Hz)

S: Section of the discharge ($10^{-4}m^2$)

j_T: Total density of current

V_D: Voltage at point D as shown in the figure 1

Consequently, the efficiency of the discharge can be calculated as the ratio between the mean UV emitted power and the mean electric power delivered to the discharge.

$$\eta_i = \frac{\int_0^T P_{i_{radiation}}(t)dt}{\int_0^T P_{i_{elec}}(t)dt} \quad (7)$$

D.1 Influence of the total pressure

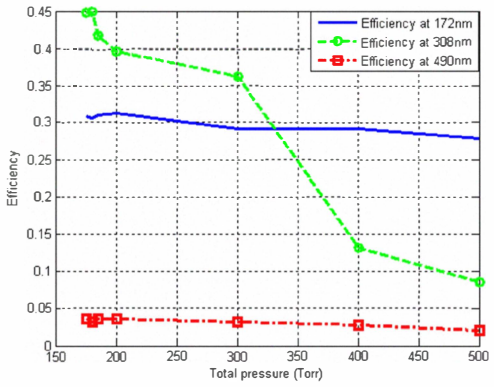

Figure 4: Influence of the total pressure on the efficiency of the XeCl excilamp supplied with a sine waveform source at V=8kV, f =50kHz and composition of Xe:Cl_2=97:3(%)

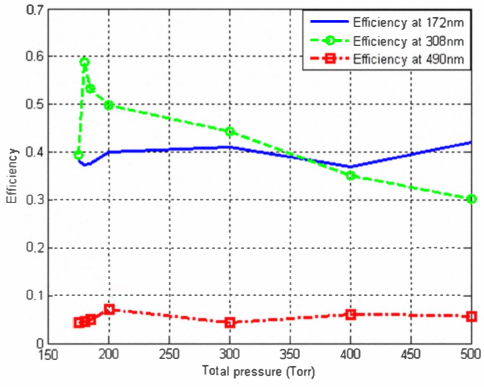

Figure 5: influence of the total pressure on the efficiency of the Xe/Cl_2 excilamp supplied with a pulsed waveform voltage source at V=8kV, f =50 kHz, duty cycle =20% and composition of Xe/Cl_2 =97:3(%)

The efficiencies of the UV radiation from the excimer of Xe^*_2 and the exciplexes of $XeCl^*$ and Xe_2Cl^* respectively η_{172}, η_{308} and η_{490} for a sine waveform voltage (V=8kV and f=50kHz) and a pulsed voltage (V=8kV, f=50kHz and duty

cycle =20%), composition of Xe/Cl_2 = 97:3(%) and P =(170-500)Torr are shown in the figures 4 and 5. It is shown that η_{308} increases with increasing of total pressure from 170Torr to 180Torr and then decreases more quickly when the total pressure continue to increase. While η_{172} and η_{490} varied also but in small range with increasing of the total pressure. Comparing the efficiencies of UV radiation between two waveforms voltages at the same conditions, we noted that the UV efficiency of a pulsed voltage is higher than a sine waveform voltage.

D.2 Influence of the Cl_2 composition

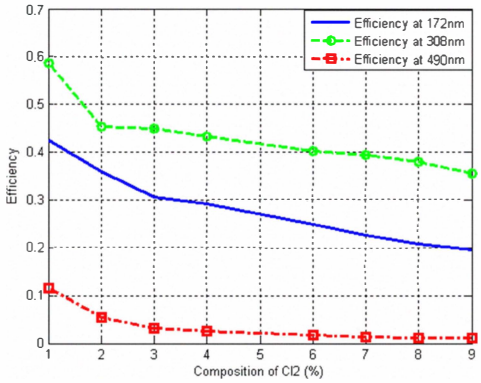

Figure 6: Influence of the Cl_2 composition on the efficiency of the Xe/Cl_2 excilamp supplied with a sine waveform voltage source at V=8kV, f=50 kHz and total pressure =180 (Torr).

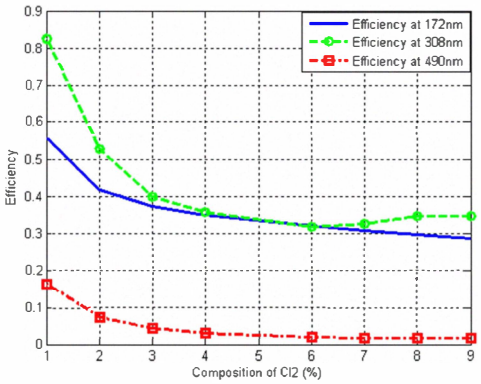

Figure 7: Influence of the Cl_2 composition on the efficiency of the Xe/Cl_2 excilamp supplied with a pulsed waveform voltage source at V=8kV, f=50 kHz, duty cycle =20%, total pressure = 180(Torr)

In figures 6 and 7, η_{172}, η_{308} and η_{490} of the Xe/Cl_2 excilamp in both two waveforms voltages show the same profile of decreasing of the UV efficiencies when increasing the composition of Cl_2 in the mixture of Xe/Cl2.

Similar to the previous results, the UV efficiencies of the Xe/Cl_2 excilamp supplied a pulsed voltage is more efficient than a sine waveform voltage as shown in the figures 6 and 7

D.3 Influence of the frequency

In this study, the voltage, the total pressure and the composition of Cl_2 is kept constant at 10kV, 180Torr and 97:3(%). The frequency of each waveform voltage varied in a range from 50 kHz to 200 kHz for a sine voltage and 50 kHz to 150 kHz for a pulsed voltage. Our obtained results are shown in the figures 8 and 9. We noted that the more the frequency increases in the case of Xe/Cl_2 supplied a sine voltage, the more η_{308} is observed. In contrast, η_{172} and η_{490} remain constant with increasing f.

In the case of the excilamp supplied with a pulsed voltage, η_{308} increases with increasing the frequency from 50 kHz to 100 kHz and achieves a maximum at 100 kHz. From this value of frequency, η_{308} decreases rapidly with increasing f. Similar to the sine voltage, η_{172} and η_{490} remain constant with the variation of the frequency.

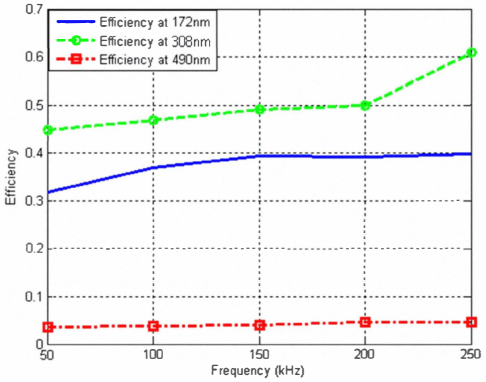

Figure 8: Influence of the frequency on the efficiency of the Xe/Cl_2 excilamp supplied with a sine waveform source at V =8kV, total pressure =180(Torr) and Compostion of Xe:Cl_2 =97:3 (%)

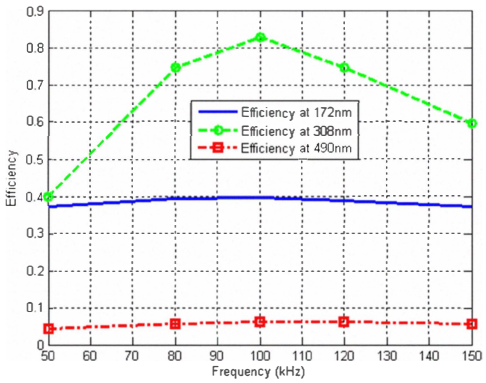

Figure 9: Influence of the frequency on the efficiency of the Xe/Cl_2 excilamp supplied with a pulsed waveform voltage source at V =8kV, total pressure =180(Torr) and composition of $Xe:Cl_2$ =97:3 (%)

D.4 Influence of the duty cycle of the pulsed voltage

The influence of the duty cycle on the UV efficiencies is presented in the figure 10. It is shown that η_{308} increases quickly with increasing the duty cycle from 10% to 40% and then keeps completely constant in a range from 50% to 60%. Beyond this last value, η_{308} decreases rapidly with increasing the duty cycle of a pulsed voltage. In contrast, there weren't significant variations in η_{172} and η_{490} when the duty cycle was changed from 10% to 80%

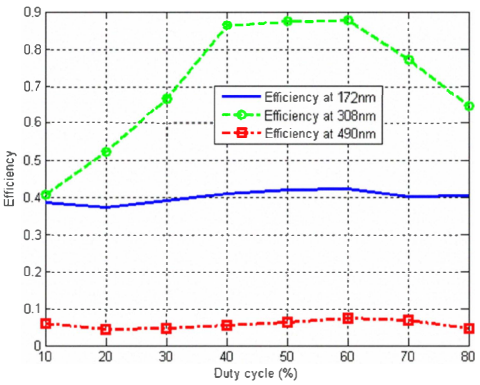

Figure 10: Influence of the duty cycle of the pulsed voltage on the efficiency of the Xe/Cl_2 excilamp

D.5 Influence of the rising time of the pulsed voltage

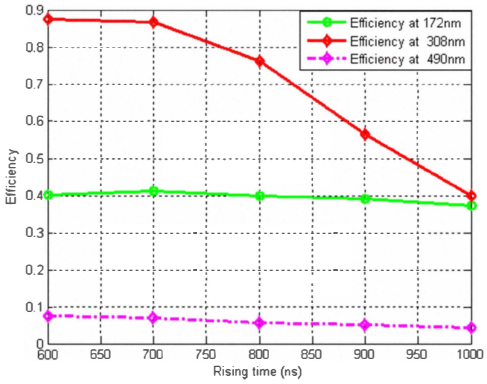

Figure 11: Influence of the rising time of the pulsed voltage on the efficiency of the Xe/Cl_2 excilamp

To evaluate the influence of the rising time of a pulsed voltage on the UV efficiencies, we fixed the following parameters: V=8kV, f=50 kHz, total pressure =180Torr, duty cycle = 20% and composition of Xe/Cl_2 = 97:3(%) and varied the rising time in a range from 1000ns to 600ns. This last value corresponds to the inferior limit value for our model. Beyond this value, if we continue to decrease the rising time, our model doesn't converge because the approximation of local field isn't correct.

The figure 11 shows that decreasing the rising time is leading to a drastic increase of the efficiency η_{308}

It is clearly shown that η_{308} at 600ns is two times higher than at 1000ns. In contrast, η_{172} and η_{490} don't have a significant variation when changing the rising time.

V. CONCLUSION

XeCl dielectric barrier discharges were simulated using one –dimensional drift diffusion model under the application of pulsed and sinusoidal voltages waveforms. It was shown that the spatiotemporal profiles of the excimers and exciplexes are mainly produced near the barrier walls at each haft cycle. At the same parameters such as the amplitude, the frequency, total pressure, rate of mixture Xe/Cl_2…etc, the light output efficiencies η_{172}, η_{308} and η_{490} for a pulse voltage are more effective than the ones of a sine voltage. The present results suggested that the light output efficiency of a DBD depend not only the power supply and also the composition of gas mixture. These results obtained in this paper help us in the design of innovative power supply topologies in order to achieve a high level of UV power and efficiency of excilamps

REFERENCES

[1] H. Akashi, Y. Sakai, N. Takahashi and T. Sasaki , "Modelling of the initiation and development of a filamentary discharge in XeCl excimer lasers", *J.Phys.D : Appl.Phys.32*, pp.2861-2870, 1999.

[2] S. Bhosle, R. Diez, H. Piquet, D. Le Thanh, B. Rahmani and D. Buso, "Modeling of a dielectric barrier discharge lamp for UV production", *Comsol conference*, Hanover, 2008.
[3] The Bolsig +, the Siglo Database,CPAT and Kinema Software, 1995..
[4] B. Eliasson, U. Kogelschatz , "Modeling and applications of silent discharge plasmas", *IEEE Transaction on Plasma science*, Vol.19, pp.309-323, Apr 1991.
[5] V. Erofeev and V. F. Tarasenko, "XeCl-, KrCl-, XeBr- and KrBr-excilamps of the barrier discharge with the nanosecond pulse duration of radiation", *J. Phys. D:Appl.Phys.39*, pp.3609-3614, Aug 2006.
[6] M. V. Erofeev, V. S. Skakun, E. A. Sonin, V. F. Tarasenko et E. B. Chernov, "Lifetime of working mixtures of XeCl and KrCl excilamps, *Atmos.Oceanic Opt*, vol.13, 2000.
[7] X. Jinzhou, G. Ying, X. Lei and Z. Jing, "Discharge transitions between glow-like and filamentary in a xenon/chlorine –filled barrier discharge lamp", *Plasma Sources Sci.Technol.*16, pp.448-453, 2007.
[8] C. Lee, M. A. Lieberman, "Global model of Ar, O_2, Cl_2 and Ar/O_2 high density plasma discharges", *Journal. Vac. Sci.Technol A*, vol.13(2),pp. 368-380, 1995.
[9] T.Letardi, H. Fang and S. Fu , "Theoretical modeling of an X-ray preionized self sustained XeCl laser ", , *IEEE journal of Quantum electronics*, Vol. 28, pp. 1647-1652, July 1992.
[10] M. I. Lomaev, E.A. Sosnin, V. F. Tarasenko, D. V. Shits, V.S.Skakun, M. V. Erofeev and A. A. Lisenko, "Capacitive and barrier discharge excilamps and their applications", , *Instruments and experimental techniques*, Vol.49, pp.595-616, 2006.
[11] J. P. Meek, L. B. Loeb , "The mechanism of the lighting discharge", *American Physical Society*, vol. 55, pp. 972-977, 1939.
[12] A. Oda, Y. Sakai, H. Akashi, H. Sugawara, "One-dimensional modelling of low frequency and high-pressure Xe barrier discharges for the design of excimer lamps", *J. Phys. D: Appl. Phys*, vol. 32, pp. 2726-2736, 1999.
[13] A. N. Panchenko, E. A. Sosnin, V. F. Tarasenko, "Improvement of output parameters of glow discharge UV excilamps", *Optics Communications 161*, pp. 249-252, 1999.
[14] L. Stafford, J. Q. Margot, F. Vidal, M. Chaker, K. Giroux, J. S. Poitier, A. Q. Leonard and J. Saussac, '' Kinetics driving chlorine high density plasmas'', *J. Appl. Phys* , vol.98, pp. 063301 – 063301-11, 2005.